



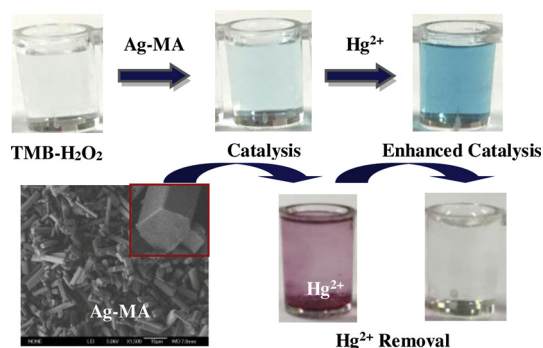
A selective colorimetric and efficient removal strategy for mercury (II) using mesoporous silver-melamine nanocomposites synthesized by controlled supramolecular self-assembly



Huan Liu, Shuai Li, Luping Feng, Yue Hua, Yuanyuan Cai, Mengyuan Yin, Yuqi Wan, Hua Wang^{*,1}

Rizhao Key Laboratory of Marine Medicine and Materials Applied Technologies, College of Chemistry and Chemical Engineering, Qufu Normal University, Qufu City, Shandong Province, 273165, PR China

GRAPHICAL ABSTRACT



ARTICLE INFO

Editor: Rinklebe Jörg

Keywords:

Ag-MA nanocomposites
Supramolecular self-assembly
Peroxidase-like catalysis
Colorimetric assay
Hg²⁺ removal

ABSTRACT

Mesoporous silver-melamine (Ag-MA) nanocomposites were synthesized by controlled supramolecular self-assembly with various structural morphologies. It was discovered that the rod-like Ag-MA nanocomposites could present the larger Hg²⁺-enhanced catalysis by forming Ag-Hg alloys. Also, they could display large surface-to-volume area and high aqueous stability for the selective Hg²⁺ enrichment and absorption of Hg²⁺ ions by yielding the stable coordination complexes. A catalysis-based colorimetric method was thus developed using 96-wells plates to probe Hg²⁺ ions in blood and wastewater with the linear Hg²⁺ concentrations ranging from 1.0 nM to 600 nM and 0.50 nM to 700 nM, respectively. Besides, mesoporous Ag-MA adsorbents could facilitate the removal of Hg²⁺ ions in wastewater with the removal efficiency up to 99.76 % and the absorption capacity of 598.99 mg g⁻¹.

1. Introduction

Heavy metal pollution has received increasing concerns throughout

the world because of the adverse effects on the environment and especially human health (Fu et al., 2012; Nolan and Lippard, 2008). Mercury (II) (Hg²⁺) as one of the most toxic heavy metals can

* Corresponding author.

E-mail addresses: huawang@qfnu.edu.cn, huawang_qfnu@126.com (H. Wang).

¹ Web: <http://wang.qfnu.edu.cn>.

extensively exist in air, water, soil, and food (Prasad et al., 2018; Ke et al., 2011; Khamdabsag et al., 2018). The accumulation of Hg^{2+} ions in human body can severely damage the digestive, excretory, and even central nervous systems, resulting in a variety of serious diseases such as muscle coordination loss, motion disorders, and endocrine system damage (Dai et al., 2018; Zhang et al., 2014). Nowadays, Hg^{2+} ions have been targeted by numerous modern detection methods such as mass spectrometry, electrochemical detection, fluorimetric analysis, and colorimetric assay (Yang et al., 2014; Xie et al., 2010; Annadhasan et al., 2014; Sun et al., 2014; Queipo Abad et al., 2017). However, most of the current methods might suffer from some disadvantages like low detection sensitivity, time-consuming, and poor analysis selectivity against the background interferences. Therefore, it is of great interest to develop a rapid, sensitive, and selective detection method for Hg^{2+} ions especially those in the complicated media like blood and wastewater.

Recent years have witnessed the direct detections of small molecular analytes (i.e., H_2O_2 and glucose) and heavy metal ions based on the specific inhibition or stimulation of catalysis (Sun et al., 2014; Jv et al., 2010; Wang et al., 2014a; Huang et al., 2018). Such a catalysis-based methodology may circumvent some limitations of the traditional detection methods (i.e., the fluorimetric ones) in terms of the sensing selectivity against the interferences of the background substances in complicated media. Moreover, nanoscaled materials of noble metals like Au or Ag nanoparticles (NPs) have concentrated numerous interests in the biochemical sensing applications due to their fantastic physicochemical properties like the enzyme-like catalysis properties (Sun et al., 2014; Zhu et al., 2013; Juan et al., 2011; Zhang et al., 2018). For example, Li et al. have synthesized AuNPs with peroxidase-like catalytic activity for sensing H_2O_2 and glucose (Jv et al., 2010). Additionally, it is widely recognized that AgNPs may present some advantages over AuNPs like cost-effectiveness, however, they may notoriously encounter with the inherent instability and poor catalytic performances, which can prevent them from the applications on a large scale. In recent years, our group have continuously devoted efforts in the preparations of various stable nanomaterials of noble metals including AgNPs alternatively by using some functional materials like polymers or metal organic frameworks (Liu et al., 2017; Fan et al., 2018; Feng et al., 2018). For example, melamine (MA) was utilized to synthesize AgNPs for sensing sulfides (Liu et al., 2017). It was well established that MA can exhibit the strong absorption capacity for various heavy metal ions (Tan et al., 2013; Zhao et al., 2015; Ge et al., 2016). For example, Zhang's group fabricated a MA-formaldehyde polymer to remove toxic metal ions from water (Tan et al., 2013). Ge et al. reported the preparation of MA-based covalent organic frameworks for the selective removal of Hg^{2+} ions through the strong MA- Hg^{2+} interaction, in which the Hg^{2+} -absorptive capacity was comparably confirmed to be over 25 times than those of other heavy metal ions like Zn^{2+} and Pb^{2+} ions (Ge et al., 2016).

In the present work, mesoporous silver-melamine (Ag-MA) nanocomposites were synthesized by the controlled supramolecular self-assembly towards a catalysis-based strategy for the selective colorimetric analysis and efficient removal of Hg^{2+} ions. It was discovered that AgNPs of the Ag-MA nanocomposites could display the Hg^{2+} -enhanced catalytic activity. Moreover, the as-prepared mesoporous nanocomposites could present large surface-to-volume area and high aqueous stability so as to enable the selective Hg^{2+} enrichment and large absorption of Hg^{2+} ions. The catalysis-based colorimetric analysis and / or efficient removal of Hg^{2+} ions from complicated media like blood and wastewater are demonstrated in detail.

2. Experiment section

2.1. Materials and instruments

Melamine (MA), silver nitrate, triphenylphosphine (PPh_3), 3, 3', 5, 5'-Tetramethylbenzidine (TMB) TMB- H_2O_2 chromogenic substrates and

dithizone were purchased from Sinopharm Chemical Reagent Co. (China). Dimethyl sulphoxide (DMSO), dithizone, citric acid, phosphate buffer solution, sodium dihydrogen phosphate, hydrogen peroxide (30%), cadmium nitrate, zinc nitrate, nickel nitrate, lead nitrate, magnesium nitrate, mercuric nitrate, chromium nitrate, and mercuric nitrate were obtained from Aladdin Reagent Co., Ltd. (Shanghai, China). Blood samples were kindly provided by the local hospital. All other reagents are of analytical grade. Deionized water ($> 18 \text{ M}\Omega$, RNase-free) was obtained from an Ultrapure water system (Pall, USA).

The colorimetric measurements of catalytic reaction products were performed by a microplate reader (Infinite M200 PRO, Tecan, Austria) with 96-well plates (JET BIOFIL, Guangzhou, China). UV-vis absorption spectra were collected using UV-3600 spectrophotometer (Shimadzu, Japan). Moreover, scanning electron microscope (SEM, JSM-6700 F, Japan) and Transmission electron microscope (TEM, JEM-2100PLUS, Japan) were employed to characterize the resulting surfaces of Ag-MA nanocomposites with and without Hg^{2+} ions. Elemental mapping measurements were conducted using a scanning electron microscope (SEM, Hitachi E-1010, Horiba Ex-250). The characterization of Ag-MA nanocomposites with different morphologies depending on the Ag-to-MA molar ratios was performed by inverted fluorescence microscope (Olympus, IX73-DP80, Japan).

2.2. Synthesis of Ag-MA nanocomposites

The Ag-MA nanocomposites were synthesized by the controlled supramolecular self-assembly procedure using silver nitrate and MA at different molar ratios. Briefly, MA (10 mM) was prepared using an aliquot of 12.6 mg of MA dissolved in 10 mL of water at 60 °C and cooled to room temperature. Under stirring, 10 mL of silver nitrate of different concentrations (5.0, 10, 20, 30, and 40 mM) was separately added into 10 mL of MA (10 mM) to be aged for 1 h, followed by the centrifugation for about 15 min at 4000 rpm, and then washing with water and alcohol, each for three times. Subsequently, Ag-MA nanocomposites were dried under vacuum to be stored in the dark. Of note, the rod-like Ag-MA nanocomposites were synthesized at the optimized Ag-to-MA molar ratio of 3/1.

2.3. Preparation of blood samples

Blood samples, which were provided by the University Hospital by collecting from healthy volunteers with informed consent, were prepared by the protein precipitation route. Briefly, an aliquot of 500.0 μL of collected blood was vigorously mixed with 40.0 μL of 0.20 M HCl and 20.0 μL PPh_3 of 0.40 M in water/acetonitrile of 20/80. After incubation for 15 min, the hydrolysed blood was mixed with 500.0 μL of acetonitrile to precipitate proteins, followed by centrifugation at 4000 rpm for 20 min. The so obtained supernatants were used further for the Hg^{2+} analysis. In addition, all the experiments were performed in compliance with the Ethical Committee Approval of China, and approved by the ethics committee at Qufu Normal University.

2.4. Colorimetric analysis of mercury

The colorimetric measurements were carried out for the Ag-MA nanocomposites with and without Hg^{2+} ions. Typically, an aliquot of 5.0 μL Ag-MA nanocomposites (5.0 mg mL^{-1}) and Hg^{2+} ions (500 nM) were introduced into the TMB- H_2O_2 substrates at room temperature for 20 min, comparing with Ag-MA nanocomposites alone, of which the blue reaction products were monitored with the UV-vis absorbance values recorded at 652 nm using 96-well plates and a microplate reader. Moreover, the detection conditions for Hg^{2+} ions were colorimetrically optimized using different Ag-MA concentrations (0.50–3.5 mg mL^{-1}), reaction time (1.0–20 min), pH values (2.0–12) and temperature (0–60 °C). Comparable studies on the peroxidase-like activities of Ag-MA nanocomposites were performed among different ions including

Zn²⁺, Na⁺, Mg²⁺, Cu²⁺, K⁺, Pb²⁺, Fe³⁺, Co²⁺, Ni²⁺, Ba²⁺, Ca²⁺, C₂O₄²⁻, SCN⁻, S²⁻, SiO₃²⁻, PO₄³⁻, NO₃⁻, SO₄²⁻, Cl⁻, F⁻, I⁻ (each 5.0 × 10⁻⁵ M), and Hg²⁺ ions (5.0 × 10⁻⁷ M).

Under the optimized conditions, the colorimetric detections of Hg²⁺ ions in buffer were conducted by following a similar procedure. First, an aliquot of Ag-MA nanocomposites (5.0 mg mL⁻¹) was separately added to TMB-H₂O₂ solutions with different concentrations of Hg²⁺ ions (0.10, 10, 50, 100, 200, 300, 400, 500, 600, and 700 nM). The mixtures were incubated at room temperature for 15 min and measured by a UV-vis absorbance at 652 nm using 96-well plates and a microplate reader. Besides, by following the same analysis procedure, different concentrations of Hg²⁺ ions spiked separately in blood (1.0, 10, 20, 50, 100, 200, 300, 400, 500, and 600 nM) and wastewater samples (0.50, 5.0, 50, 100, 200, 300, 400, 500, 600, and 700 nM) were analyzed, where the levels of Hg²⁺ ions in the raw samples were pre-determined as the blank ones.

The steady state kinetic studies were comparably carried out using Ag-MA nanocomposites in the absence and presence of Hg²⁺ ions (5.0 × 10⁻⁷ M), where 8.82 mM H₂O₂ or 0.42 mM TMB was used alternately at a fixed concentration of one substrate versus varying concentration of the second substrate of TMB (0.3, 0.4, 0.5, 0.6, 0.8, and 1.0 mM) or H₂O₂ (1.7, 3.3, 5.0, 10, 20, 25, and 50 mM). Subsequently, dynamics parameters of catalysis activities of Ag-MA nanocomposites in the absence and presence of Hg²⁺ ions were calculated by double-reciprocal plotting, including the Michaelis constant (K_m) and the maximal reaction velocity (V_{max}).

2.5. Absorption experiments for metal ions

The absorption performances of Ag-MA nanocomposites for Hg²⁺ ions were examined by comparing with other kinds of metal ions of Cd²⁺, Zn²⁺, Ni²⁺, Pb²⁺, Mg²⁺, Cu²⁺, and Cr³⁺ ions. Typically, under the stirring conditions, an aliquot of Ag-MA nanocomposites (10 mg) was separately added into 10 mL of each of metal ions-containing solutions (600.40 mg L⁻¹, pH 7.0) for 24 h at room temperature. After the separation by centrifugation, the concentrations of the left metal ions (i.e., Hg²⁺ ions) in the solutions were determined either by using atomic absorption spectrometry (Hitachi Z-2000, Japan) or the chromogenic reactions (i.e., 0.0050 g mL⁻¹ dithizone for Hg²⁺ ions). The absorption capacities and removal efficiencies of metal ions were further calculated by the following equations, in which C₀ and C_e represent the initial and final concentrations of metal ions, respectively:

$$\text{Absorption capacity} = C_0 - C_e \quad (1)$$

$$\text{Removal efficiency (\%)} = (C_0 - C_e)/C_0 \times 100 \% \quad (2)$$

Besides, the absorption capacities of Ag-MA nanocomposites for Hg²⁺ ions with different concentrations (600.40, 521.10, 98.90, 50.00, 10.90, 2.11, 0.50 and 0.10 mg L⁻¹) spiked in wastewater samples were determined accordingly.

3. Results and discussion

3.1. Main principle and procedure for the analysis and removal of Hg²⁺ ions

Scheme 1 schematically illustrates the fabrication procedure of Ag-MA nanocomposites for the catalysis-based colorimetric analysis and absorption-based removal of Hg²⁺ ions. Herein, mesoporous Ag-MA nanocomposites were synthesized simply by the controlled supramolecular self-assembly process using silver nitrate and MA precursors (Scheme 1A). It was found that AgNPs in the resulting Ag-MA nanocomposites display a low peroxidase-like catalytic activity in catalyzing 3, 3', 5, 5'-tetramethylbenzidine (TMB)-H₂O₂ reactions, which could be dramatically enhanced once Hg²⁺ ions were introduced, showing the deep blue reaction products (Scheme 1B). Furthermore, the mesoporous

Ag-MA nanocomposites were employed for the absorption-based removal of Hg²⁺ ions. As expected, Ag-MA nanocomposites with high surface-to-volume area could conduct an efficient absorption for Hg²⁺ ions through the strong interactions between nitrogen groups-containing MA and Hg²⁺ ions to yield the extremely stable coordination complexes, which may lead to the aggregation of Ag-MA nanocomposites (Ge et al., 2016; Guoyan et al., 2014). More importantly, the formation of Ag-Hg alloys would change the surface properties of AgNPs in the nanocomposites (Sun et al., 2014; Wang et al., 2014b), so that the Hg²⁺-enhanced catalysis of AgNPs in nanocomposites could thereby be triggered towards the visual colorimetric analysis of Hg²⁺ ions in addition to the efficient removal afterwards.

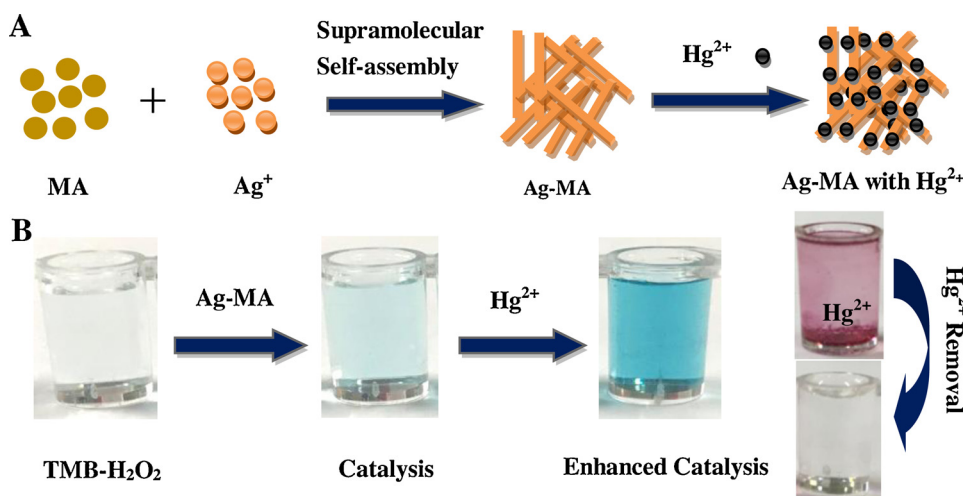
3.2. Characterization of Ag-MA nanocomposites

The changing topological structures of Ag-MA nanocomposites in the absence and presence of Hg²⁺ ions were characterized using scanning electron microscope (SEM) and transmission electron microscope (TEM) (Fig. 1). One can note from Fig. 1A that the original products of Ag-MA nanocomposites could exhibit uniform rod-like profile with the side width of about 2.5 μm, with the mesoporous structure as revealed in the amplified view (insert), which could also be witnessed clearly from the TEM images (Fig. 1C). Importantly, this controlled supramolecular self-assembly could enable the Ag-MA nanocomposites to be formed with well defined mesoporous structures, as clearly shown in the amplified view (insert), so as to expect the high surface-to-volume ratio for the large-scale absorption of targeting substances (i.e., Hg²⁺ ions). Meantime, the morphological structure of Ag-MA nanocomposites after the introduction of Hg²⁺ ions was characterized by SEM imaging. To our surprise, the Ag-MA nanocomposites could be broken in the presence of Hg²⁺ ions to yield the large aggregation blocks (Fig. 1B), as apparently shown in the amplified view of one particle (insert). Additionally, Fig. 1D indicates that the Ag-Hg alloys might be formed in the resultant products (black coagulations), as revealed in the amplified view (insert). Such a phenomenon might be attributed to the strong interaction between Hg²⁺ ions and amino groups of the MA-containing nanocomposites, so as to facilitate the efficient absorption-based removal of Hg²⁺ ions from wastewater samples afterwards.

In addition, the chemical composition of the resulting Ag-MA-Hg²⁺ composites was analyzed by elemental mapping (Fig. 2). It was found that C, N, Ag, and Hg elements could be uniformly dispersed in the Ag-MA matrix in a discretely mixed way, indicating that Hg²⁺ ions could be efficiently absorbed by the Ag-MA nanocomposites as expected. Moreover, morphological investigations were conducted comparably for the Ag-MA nanocomposites prepared at different Ag-to-MA ratios by microscopy imaging (Fig. 3). Obviously, the structural morphologies of Ag-MA nanocomposites could depend on the Ag-to-MA ratios used in the controlled supramolecular self-assembly process (Fig. 3A-E). One can note that rod-like Ag-MA nanocomposites can be obtained at the Ag-to-MA ratios of 4/1 and 3/1 (Fig. 3A-B). With the increasing amounts of MA, the rod-like nanocomposites could be gradually lessened and the wire-like ones could be further formed (Fig. 3C-E). More importantly, Fig. 3F manifests that the biggest Hg²⁺-enhanced catalysis could be obtained for the AgNPs in rod-like Ag-MA nanocomposites that were fabricated at the Ag-to-MA ratio of 3/1, which was thus selected for the selective colorimetric assays of Hg²⁺ ions afterwards.

3.3. Analysis performances of Ag-MA nanocomposites for sensing Hg²⁺ ions

The mercury (II)-enhanced catalysis of AgNPs in the rod-like Ag-MA nanocomposites was comparably explored in the absence and presence of Hg²⁺ ions (Fig. 4A). It was found that AgNPs in the nanocomposites could display a considerably low catalytic activity in the TMB-H₂O₂ reactions forming the light blue products. In contrast, the addition of



Scheme 1. Schematic illustration of (A) the synthesis procedure of Ag-MA nanocomposites for sensing Hg^{2+} ions and (B) the colorimetric and removal protocol of Hg^{2+} ions using Ag-MA nanocomposites with Hg^{2+} -enhanced catalytic activity in catalyzing the TMB- H_2O_2 reactions and Hg^{2+} absorption, showing the changing colors of reaction solutions.

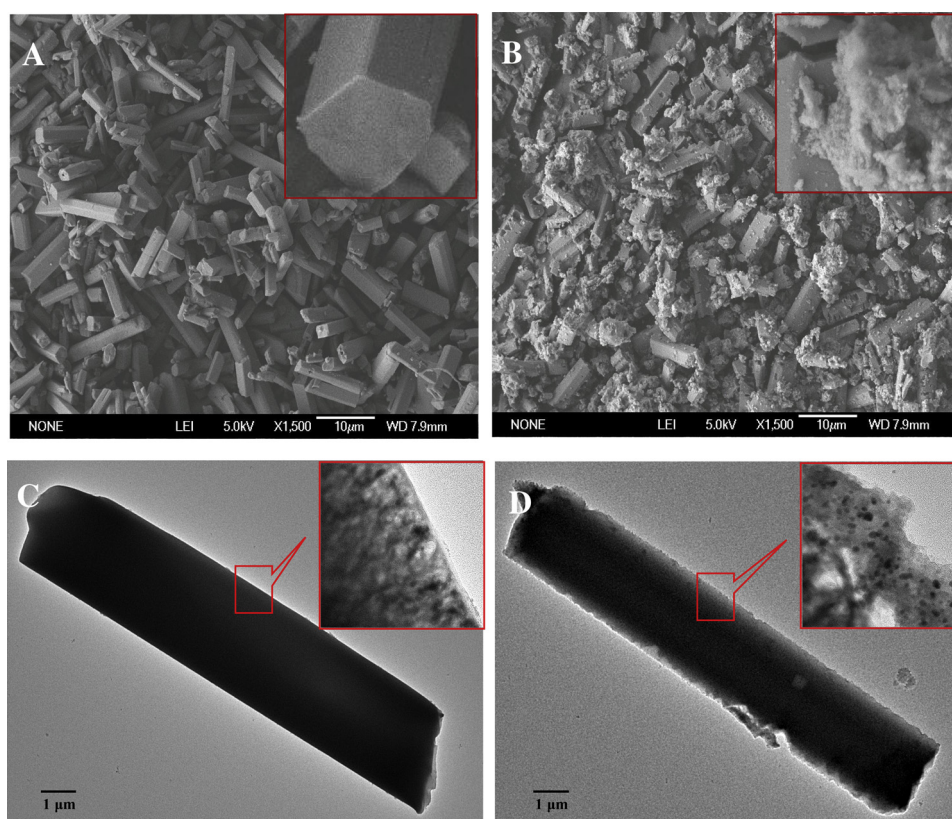


Fig. 1. SEM images and TEM images of Ag-MA nanocomposites (A, C) before and (B, D) after adding Hg^{2+} ions (insert: the amplified views).

Hg^{2+} ions could significantly enhance the catalytic activity of AgNPs in Ag-MA nanocomposites, showing the deep blue products of TMB- H_2O_2 reactions (insert, Fig. 4A). Furthermore, the effects of some other ions on the catalytic activities of Ag-MA nanocomposites were investigated (Fig. 4B). One can observe that these common inorganic ions might present the negligibly low stimulation for the catalysis of AgNPs in Ag-MA nanocomposites, even with the concentrations of 100-fold higher than that of Hg^{2+} ions. The above facts prove that Hg^{2+} ions could specifically facilitate the enhanced catalysis of AgNPs in Ag-MA nanocomposites presumably due to the formation of Ag-Hg alloys that might change the surface properties of catalytic AgNPs in nanocomposites aforementioned. Yet, the detailed mechanism should be further investigated in the future. A label-free visual colorimetric protocol has thus been proposed for the selective detection of Hg^{2+}

ions by taking the advantage of the catalysis enhancement of AgNPs in Ag-MA nanocomposites through circumventing any interference from other metal ions. Moreover, a UV-vis spectrophotometer was utilized to characterize Ag-MA nanocomposites before and after adding Hg^{2+} ions (Fig. S1). It was observed from Fig. S1A that the addition of Hg^{2+} ions could decrease the UV-vis absorbance of Ag-MA nanocomposites. Interestingly, the nanocomposite suspensions could become clear in the presence of Hg^{2+} ions, as revealed in the corresponding photographs (Fig. S1B). Therefore, the large Hg^{2+} absorption by Ag-MA nanocomposites could occur due to the powerfully strong MA- Hg^{2+} interaction (Ge et al., 2016), promising the selective enrichment and / or removal of Hg^{2+} ions from blood and wastewater.

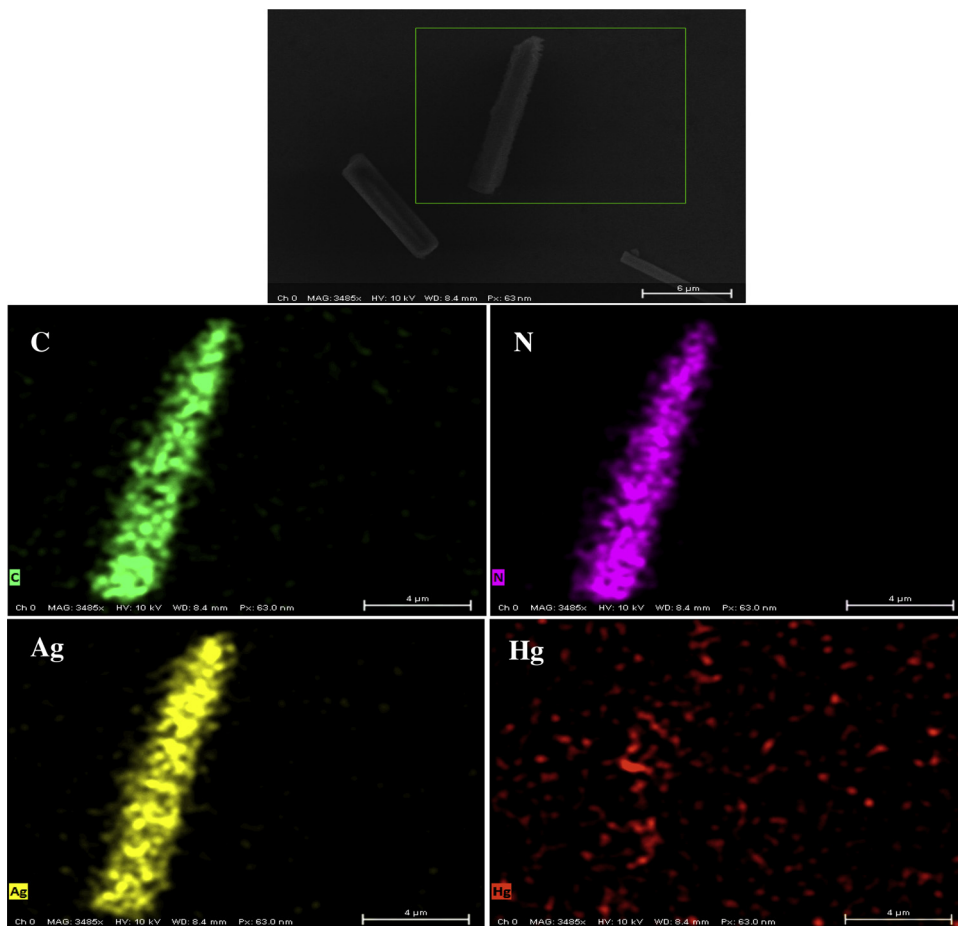


Fig. 2. Element mapping images of Ag-MA-Hg²⁺ composed of C, N, Ag and Hg elements shown in green, purple, yellow, and red colors, respectively. (For interpretation of the references to colour in this figure legend, the reader is referred to the web version of this article).

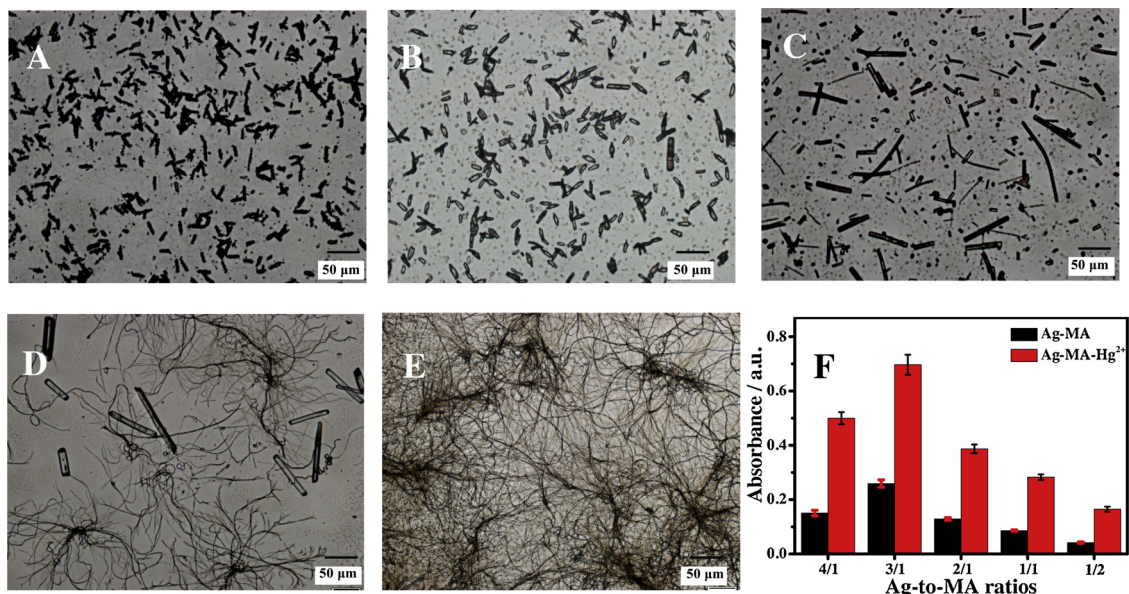


Fig. 3. Microscopy images of Ag-MA nanocomposites products synthesized at different Ag-to-MA ratios of (A) 4/1, (B) 3/1, (C) 2/1, (D) 1/1, and (E) 1/2. (F) Effects of Ag-to-MA ratios on the catalysis activities of Ag-MA nanocomposites in sensing Hg²⁺ ions by catalyzing the TMB-H₂O₂ reactions, with the photographs of Ag-MA product solutions (insert).

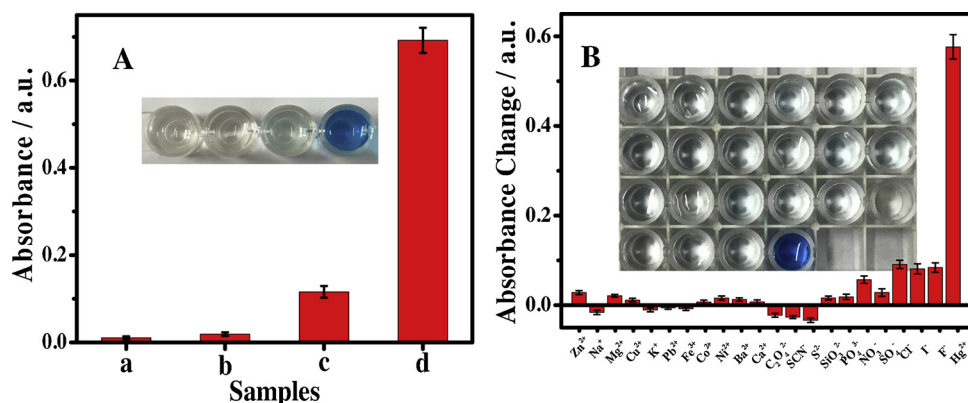


Fig. 4. Comparable investigations on (A) the peroxidase-like catalysis activities of AgNPs in Ag-MA nanocomposites (c) without and (d) with Hg^{2+} ions, taking (a) TMB- H_2O_2 and (b) Hg^{2+} ions as the controls, and (B) Ag-MA mixed separately with different cations (Zn^{2+} , Na^+ , Mg^{2+} , Cu^{2+} , K^+ , Pb^{2+} , Fe^{3+} , Co^{2+} , Ni^{2+} , Ba^{2+} , Ca^{2+} , and Hg^{2+} ions) or anions ($\text{C}_2\text{O}_4^{2-}$, SCN^- , S^{2-} , SiO_3^{2-} , PO_4^{3-} , NO_3^- , SO_4^{2-} , Cl^- , F^- , and I^- ions), with the photographs of corresponding product solutions of catalytic TMB- H_2O_2 reactions (insert).

3.4. Colorimetric sensing properties of the Ag-MA nanocomposites

The catalysis dynamics of AgNPs in Ag-MA nanocomposites was comparably investigated in the absence and presence of Hg^{2+} ions (Fig. S2). Herein, colorimetric measurements were performed alternatively for different concentrations of TMB and H_2O_2 to obtain the Michaelis-Menten curves (Gao et al., 2007). By comparison, the Ag-MA nanocomposites with Hg^{2+} ions could present much lower Michaelis constant (K_m) for the catalytic reaction substrates of TMB (Fig. S2A) or H_2O_2 (Fig. S2B). Much larger values of maximal reaction velocity (V_{max}) could also be expected for the Hg^{2+} -containing Ag-MA nanocomposites. Accordingly, Hg^{2+} ions could significantly enhance the catalytic activity of AgNPs in Ag-MA nanocomposites showing the higher affinities both to TMB and H_2O_2 . Importantly, the colorimetric analysis of Hg^{2+} ions could thus be achieved on the basis of the Hg^{2+} -enhanced catalysis of AgNPs in Ag-MA nanocomposites.

Furthermore, studies were made on the storage stability of the developed Ag-MA nanocomposites (Fig. 5A). As expected, no significant change in the colorimetric responses was recorded for Hg^{2+} ions using Ag-MA nanocomposites stored in dark even up to six months. Also, the colorimetric reproducibility of Ag-MA nanocomposites for sensing Hg^{2+} ions was investigated (Fig. 5B). One can note that the developed method could display basically consistent Hg^{2+} responses among the several detections. These results indicate that the developed colorimetric method with Ag-MA nanocomposites could promise high reproducibility for the detection of Hg^{2+} ions.

3.5. Optimization of colorimetric Hg^{2+} conditions

The effects of analysis conditions on the performances of the Ag-MA nanocomposites-based colorimetric method for sensing Hg^{2+} ions were investigated, mainly including the Ag-MA nanocomposites concentrations, reaction time, pH values, and temperature (Fig. S3). As shown in Fig. S3A, the colorimetric responses to Hg^{2+} ions can increase with

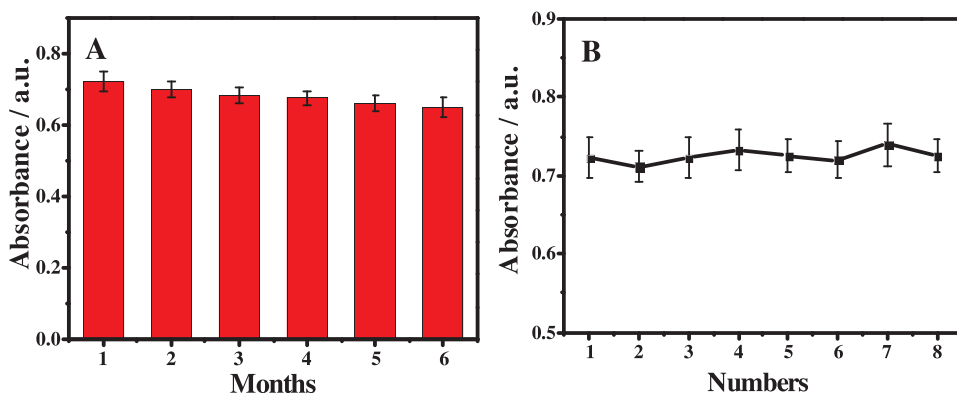


Fig. 5. (A) The storage stability of Ag-MA nanocomposites for the colorimetric Hg^{2+} analysis, which were separately stored in dark for different time intervals before the Hg^{2+} detections. (B) The analysis reproducibility of the developed colorimetric method for sensing Hg^{2+} (600 nM) based on the Hg^{2+} -enhanced catalysis activities of Ag-MA nanocomposites.

increasing dosages of Ag-MA nanocomposites till 2.5 mg mL^{-1} , over which the signals would be unchanged. The phenomenon may presumably be attributed to the fact that much denser Ag-MA nanocomposites might react with Hg^{2+} ions leading to the stable signals. Accordingly, 2.5 mg mL^{-1} of Ag-MA nanocomposites was thought to be the optimal one in the experiments. Fig. S3B shows that the reaction time of the colorimetric analysis of Hg^{2+} ions, revealing that the Hg^{2+} ions response could be completed within 15 min. Meanwhile, as clearly disclosed in Fig. S3C, pH values could influence the colorimetric analysis of Hg^{2+} ions responses. Obviously, the highest response could be obtained at pH 6.0, which should be selected as the most suitable one. Fig. S3D exhibits that the responses could increase as temperature increasing up to 37°C , over which the responses could gradually decrease. Accordingly, 37°C was thus chosen as the optimal one for sensing Hg^{2+} ions. It should be pointed out that the used suspensions of Ag-MA nanocomposites might be disassembled by heating over 60°C to dissolve MA, which might be re-assembled as the temperature decreased down to room temperature (i.e., 20°C) (Fei et al., 2013).

3.6. Analysis of Hg^{2+} ions in samples

Under the optimized conditions, the developed Ag-MA nanocomposites-based colorimetric method was employed to practically probe Hg^{2+} ions with different concentrations in various samples using 96-well plates (Fig. 6). Fig. 6A illustrates the calibration detection curve for Hg^{2+} ions in buffer, showing the linear detection range of Hg^{2+} concentrations from 0.10–700 nM with the limit of detection (LOD) of 0.025 nM as estimated by the 3σ rule. Such a LOD is lower than those of the other detection methods reported previously (Xie et al., 2010; Juan et al., 2011; Wang et al., 2014b; Zhang et al., 2013). Moreover, the colorimetric assays were conducted for Hg^{2+} ions with various levels separately spiked in blood (Fig. 6B) and wastewater (Fig. 6C), showing the linear Hg^{2+} concentrations ranging from 1.0 nM to 600 nM and 0.50 nM to 700 nM with LODs of 0.33 nM and 0.18 nM, respectively.

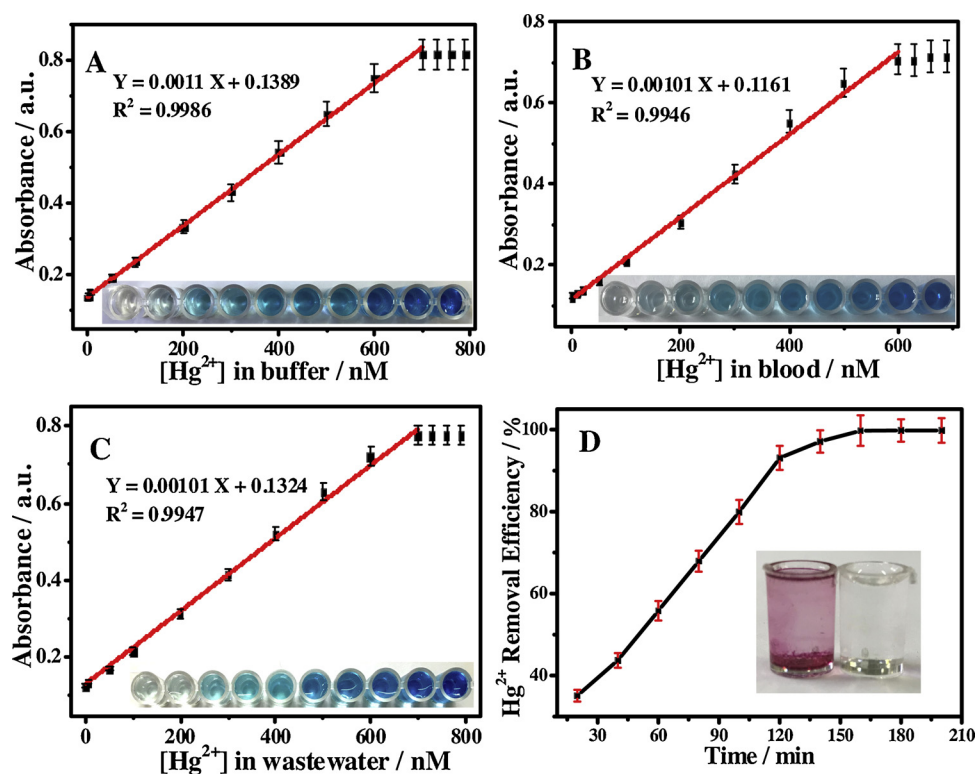


Fig. 6. Calibration detection curves for the linear relationship of absorbance values vs. different concentrations of Hg^{2+} ions spiked in (A) buffer, (B) blood and (C) wastewater samples, with the photographs of corresponding product solutions of catalytic reactions (insert). (D) The time-dependent removal efficiencies of Hg^{2+} ions ($600.40 \text{ mg mL}^{-1}$), with the photographs of chromogenic reactions with dithizone before (left) and after (right) the removal of Hg^{2+} ions (insert).

Therefore, the catalysis-based colorimetric assay can detect Hg^{2+} ions in complicated samples with high analysis sensitivity and selectivity. In addition, the recovery tests were also performed by using the developed colorimetric method to probe Hg^{2+} ions in wastewater samples, showing the recoveries obtained ranging from about 98.15–105.1 % (Table S1).

3.7. Removal of Hg^{2+} ions in wastewater

The absorption-based removal efficiencies of Ag-MA nanocomposites for mercury in industrial wastewater were explored (Fig. 6D). One can note that the Hg^{2+} -removal efficiencies can depend on the time of absorption reactions, which can be basically finished within 160 min to show a clear product solution of the chromogenic reactions using dithizone, as visually seen from the photographs (insert). Moreover, the absorption and removal performances of Ag-MA nanocomposites were explored for Hg^{2+} ions with different concentrations in wastewater samples, with the results shown in Table 1. It was discovered that Ag-MA nanocomposites could achieve the removal of Hg^{2+} ions with the efficiency up to 99.76 % and the absorption capacity of 598.99 mg g^{-1} for the high Hg^{2+} concentration (600.40 mg L^{-1}). Also, a removal efficiency up to 91.58 % could be attained for the low Hg^{2+}

Table 1

The results of absorption and removal performances of Ag-MA nanocomposites for Hg^{2+} ions with different concentrations in wastewater samples.

Hg^{2+} concentrations (mg L^{-1})		Absorption capacities (mg g^{-1})	Removal efficiencies (%)
Initial	After absorption		
600.40	1.41	598.99	99.76
521.10	1.21	519.89	99.75
98.90	0.30	98.60	99.70
50.00	0.17	49.83	99.65
10.90	0.15	10.75	98.65
2.11	0.050	2.06	97.78
0.50	0.030	0.47	93.41
0.10	0.0080	0.092	91.58

concentration (0.10 mg L^{-1}). Furthermore, the absorption capacities of Ag-MA nanocomposites were also investigated for some other kinds of metal ions (Table S2). One can note that the Hg^{2+} -absorption capacity of Ag-MA nanocomposites is over 25-fold higher than those of other kinds of metal ions like Zn^{2+} and Cu^{2+} ions, of which the capacity can be consistent with that of the previous report (Ge et al., 2016). Importantly, one can see from Table S2 that the nanocomposites could show no big change in the absorption capacity for Hg^{2+} when mixed with these tested metal ions, suggesting that these co-existing metal ions might not have any influence on the selective absorption of Ag-MA nanocomposites for Hg^{2+} ions. In addition, as aforementioned, the further improvement of the Hg^{2+} removal efficiencies of Ag-MA nanocomposites may be expected if the used nanocomposites were regenerated by heating the suspensions over 60°C to disassemble the nanocomposites, which might be re-assembled as the temperature down to room temperature. Importantly, it was experimentally found that after five runs of recycling tests, the Ag-MA nanocomposites could show no significant change in the absorption and sensing performances for Hg^{2+} ions.

Furthermore, the Hg^{2+} -removal performances of the developed Ag-MA nanocomposites were compared with those of the other kinds of documented adsorbent materials, with the results summarized in Table S3. One can note that the Hg^{2+} -removal performances of the Ag-MA nanocomposites can be better or comparable with the adsorbents previously reported in terms of removal efficiency and absorption capacity. Herein, as aforementioned, the highly efficient absorption and removal capabilities of Ag-MA nanocomposites for Hg^{2+} ions should be attributed to their mesoporous structure of high surface-to-volume area and especially the powerful Hg^{2+} -chelating ability of nitrogen-rich MA in nanocomposites forming the extremely stable coordination complexes (Ge et al., 2016; Pearson, 1988).

4. Conclusion

In summary, mesoporous Ag-MA nanocomposites were successfully synthesized simply by the controlled supramolecular self-assembly with

various structural morphologies depending on the Ag-to-MA ratios used. It was discovered that AgNPs in rod-like Ag-MA ones could display the biggest Hg^{2+} -enhanced catalytic activity, which was thought to result from the formation of Ag-Hg alloys that would change the surface properties of catalytic AgNPs in nanocomposites. A catalysis-based colorimetric protocol was thereby developed for probing Hg^{2+} ions with the levels down to 0.025 nM, showing high analysis sensitivity, selectivity, and reproducibility. Moreover, the so prepared mesoporous Ag-MA absorbents with large surface-to-volume area and high aqueous stability could enable the efficient absorption of Hg^{2+} ions, with the removal efficiency up to 99.76 % with the absorption capacity of 598.99 mg g^{-1} . Meantime, the MA-containing Ag-MA nanocomposites with rich amino groups could chemically chelate with Hg^{2+} ions so as to expect the further improved enrichment and / or removal of Hg^{2+} ions from the complicated media like blood and wastewater. Such a catalysis-based colorimetric method with mesoporous Ag-MA nanocomposites can allow for the selective monitoring and / or efficient removal of Hg^{2+} ions in some complicated samples, thus promising the huge potential applications in the clinical diagnosis, environmental monitoring, and industrial wastewater treatment fields.

Acknowledgements

This work was supported by the National Natural Science Foundations of China (No. 21675099), Major Basic Research Program of Natural Science Foundation of Shandong Province (ZR2018ZC0129), and Key R&D Plan of Jining City (2018HMNS001), Shandong, P. R. China.

Appendix A. Supplementary data

Supplementary material related to this article can be found, in the online version, at doi:<https://doi.org/10.1016/j.jhazmat.2019.121798>.

References

- Annadhasan, M., Muthukumarasamyvel, T., Sankar Babu, V.R., Rajendiran, N., 2014. Green synthesized silver and gold nanoparticles for colorimetric detection of Hg^{2+} , Pb^{2+} , and Mn^{2+} in aqueous medium. *ACS Sustain. Chem. Eng.* 2, 887–896.
- Dai, R., Deng, W., Hu, P., You, C., Yang, L., Jiang, X., Xiong, X., Huang, K., 2018. One-pot synthesis of bovine serum albumin protected gold/silver bimetallic nanoclusters for ratiometric and visual detection of mercury. *Microchem. J.* 139, 1–8.
- Fan, C., Lv, X., Liu, F., Feng, L., Liu, M., Cai, Y., Liu, H., Wang, J., Yang, Y., Wang, H., 2018. Silver nanoclusters encapsulated into metal-organic frameworks with enhanced fluorescence and specific ion accumulation toward the microdot array-based fluorimetric analysis of copper in blood. *ACS Sens.* 3, 441–450.
- Fei, J., Gao, L., Zhao, J., Du, C., Li, J., 2013. Responsive helical self-assembly of AgNO_3 and melamine through asymmetric coordination for Ag nanochain synthesis. *Small* 9, 1021–1024.
- Feng, L., Liu, M., Liu, H., Fan, C., Cai, Y., Chen, L., Zhao, M., Chu, S., Wang, H., 2018. High-throughput and sensitive fluorimetric strategy for microRNAs in blood using wettable microwells array and silver nanoclusters with red fluorescence enhanced by metal organic frameworks. *ACS Appl. Mater. Interfaces* 10, 23647–23656.
- Fu, X., Lou, T., Chen, Z., Lin, M., Feng, W., Chen, L., 2012. “Turn-on” fluorescence detection of lead ions based on accelerated leaching of gold nanoparticles on the surface of graphene. *ACS Appl. Mater. Interfaces* 4, 1080–1086.
- Gao, L., Zhuang, J., Nie, L., Zhang, J., Zhang, Y., Gu, N., Wang, T., Feng, J., Yang, D., Perrett, S., Yan, X., 2007. Intrinsic peroxidase-like activity of ferromagnetic nanoparticles. *Nat. Nanotechnol.* 2, 577–583.
- Ge, J., Xiao, J., Liu, L., Qiu, L., Jiang, X., 2016. Facile microwave-assisted production of Fe_3O_4 decorated porous melamine-based covalent organic framework for highly selective removal of Hg^{2+} . *J. Porous Mater.* 23, 791–800.
- Guoyan, L., Huipeng, R., Yuyu, G., Ronghua, D., Chunyan, C., 2014. Development of a mercury detection kit based on melamine-functionalized gold nanoparticles. *Anal. Sci.* 31, 113–118.
- Huang, Y.Q., Fu, S., Wang, Y.S., Xue, J.H., Xiao, X.L., Chen, S.H., Zhou, B., 2018. Protamine-gold nanoclusters as peroxidase mimics and the selective enhancement of their activity by mercury ions for highly sensitive colorimetric assay of $\text{Hg}(\text{II})$. *Anal. Bioanal. Chem.* 410, 7385–7394.
- Juan, L.Y., Fang, L.Y., Yue, L., Jia, Z.J., Jie, T., Zhi, H.C., 2011. Visual observation of the mercury-stimulated peroxidase mimetic activity of gold nanoparticles. *Chem. Commun.* 47, 11939–11941.
- Jv, Y., Li, B., Cao, R., 2010. Positively-charged gold nanoparticles as peroxidase mimic and their application in hydrogen peroxide and glucose detection. *Chem. Commun.* 46, 8017–8019.
- Ke, F., Qiu, L.G., Yuan, Y.P., Peng, F.M., Jiang, X., Xie, A.J., Shen, Y.H., Zhu, J.F., 2011. Thiol-functionalization of metal-organic framework by a facile coordination-based postsynthetic strategy and enhanced removal of Hg^{2+} from water. *J. Hazard. Mater.* 196, 36–43.
- Khamdagsag, P., Khemthong, P., Sittisuwannakul, K., Grisdanurak, N., Wutikhun, T., Rungnim, C., Namuangruk, S., Pimpha, N., 2018. Insights into binding mechanism of silver/titanium dioxide composites for enhanced elemental mercury capture. *Mater. Chem. Phys.* 215, 1–10.
- Liu, M., Zhang, L., Hua, Y., Feng, L., Jiang, Y., Ding, X., Qi, W., Wang, H., 2017. Mesoporous silver-melamine nanowires formed by controlled supermolecular self-assembly: a selective solid-state electroanalysis for probing multiple sulfides in hyperhaline media through the specific sulfide-chloride replacement reactions. *Anal. Chem.* 89, 9552–9558.
- Nolan, E.M., Lippard, S.J., 2008. Tools and tactics for the optical detection of mercuric ion. *Chem. Rev.* 108, 3443–3480.
- Pearson, R.G., 1988. Chemical hardness and bond dissociation energies. *J. Am. Chem. Soc.* 110, 7684–7690.
- Prasad, K.S., Shruthi, G., Shivamallu, C., 2018. Functionalized silver nano-sensor for colorimetric detection of Hg^{2+} ions: facile synthesis and docking studies. *Sensors* 18, 2698–2706.
- Queipo Abad, S., Rodríguez-González, P., Davis, W.C., García Alonso, J.I., 2017. Development of a common procedure for the determination of methylmercury, ethylmercury, and inorganic mercury in human whole blood, hair, and urine by triple spike species-specific isotope dilution mass spectrometry. *Anal. Chem.* 89, 6731–6739.
- Sun, Z., Zhang, N., Si, Y., Li, S., Wen, J., Zhu, X., Wang, H., 2014. High-throughput colorimetric assays for mercury (II) in blood and wastewater based on the mercury-stimulated catalytic activity of small silver nanoparticles in a temperature-switchable gelatin matrix. *Chem. Commun.* 50, 9196–9199.
- Tan, M.X., Sum, Y.N., Ying, J.Y., Zhang, Y., 2013. A mesoporous poly-melamine-formaldehyde polymer as a solid sorbent for toxic metal removal. *Energy Environ. Sci.* 6, 3254–3259.
- Wang, H., Li, S., Si, Y., Zhang, N., Sun, Z., Wu, H., Lin, Y., 2014a. Platinum nanocatalysts loaded on graphene oxide-dispersed carbon nanotubes with greatly enhanced peroxidase-like catalysis and electrocatalysis activities. *Nanoscale* 6, 8107–8116.
- Wang, G.-L., Xu, X.-F., Cao, L.-H., He, C.-H., Li, Z.-J., Zhang, C., 2014b. Mercury (II)-stimulated oxidase mimetic activity of silver nanoparticles as a sensitive and selective mercury (II) sensor. *RSC Adv.* 4, 5867–5872.
- Xie, J., Zheng, Y., Ying, J.Y., 2010. Highly selective and ultrasensitive detection of Hg^{2+} based on fluorescence quenching of Au nanoclusters by Hg^{2+} - Au^+ interactions. *Chem. Commun.* 46, 961–963.
- Yang, L., Zhang, C., Jiang, H., Li, G., Wang, J., Wang, E., 2014. Insertion approach: bolstering the reproducibility of electrochemical signal amplification via DNA superstructures. *Anal. Chem.* 86, 4657–4662.
- Zhang, C., Sun, X., Li, J., Liu, Y.-N., 2013. Synthesis of Ag nanoclusters by a pH-dependent etching method in aqueous solution. *Nanoscale* 5, 6261–6264.
- Zhang, N., Si, Y., Sun, Z., Chen, L., Li, R., Qiao, Y., Wang, H., 2014. Rapid, selective, and ultrasensitive fluorimetric analysis of mercury and copper levels in blood using bimetallic gold-silver nanoclusters with “silver effect”-enhanced red fluorescence. *Anal. Chem.* 86, 11714–11721.
- Zhang, X., Liu, W., Li, X., Zhang, Z., Shan, D., Xia, H., Zhang, S., Lu, X., 2018. Ultrahigh selective colorimetric quantification of chromium(VI) ions based on gold amalgam catalyst oxidoreductase-like activity in water. *Anal. Chem.* 90, 14309–14315.
- Zhao, Y., Xu, L., Li, S., Chen, Q., Yang, D., Chen, L., Wang, H., 2015. “One-drop-of-blood” electroanalysis of lead levels in blood using a foam-like mesoporous polymer of melamine-formaldehyde and disposable screen-printed electrodes. *Analyst* 140, 1832–1836.
- Zhu, R., Zhou, Y., Wang, X.L., Liang, L.P., Long, Y.J., Wang, Q.L., Zhang, H.J., Huang, X.X., Zheng, H.Z., 2013. Detection of Hg^{2+} based on the selective inhibition of peroxidase mimetic activity of BSA-Au clusters. *Talanta* 117, 127–132.